Langmuir

Article

pubs.acs.org/Langmuir

Biological Hydrogels Formed by Swollen Multilamellar Liposomes

Chih-Yang Cheng,[†] Ting-Yu Wang,[‡] and Shih-Huang Tung*[,†]

[†]Institute of Polymer Science and Engineering and [‡]Instrumentation Center, National Taiwan University, Taipei 10617, Taiwan

Supporting Information

ABSTRACT: The self-assembly of lecithin-bile salt mixtures in solutions has long been an important research topic, not only because they are both biosurfactants closely relevant to physiological functions but also for the potential biomedical applications. In this paper, we report an unusual biological hydrogel formed by mixing bile salts and lecithin at low bile salt/lecithin molar ratios (B_0) in water. The gel can be prepared at a total lipid concentration as low as ~15 wt %, and the solidlike property of the solutions was confirmed by dynamic rheological measurements. We used cryo-TEM and SAXS/SANS techniques to probe the self-assembled structure and clearly evidence that the gel is made up of jammed swollen multilamellar vesicles (liposomes), instead of typical fibrous networks found in conventional gels. A mechanism-based on the strong repulsion between bilayers due to the incorporation of negatively charged bile salts is proposed to explain the swelling of the liposomes. In addition to gel, a series of phases, including viscoelastic, gel-like, and low-viscosity fluids, can be created by increasing B_0. Such a variety of phase behaviors are caused by the transformation of bilayers into cylindrical and spheroidal micelles upon the change of the effective molecular geometry with B_0.

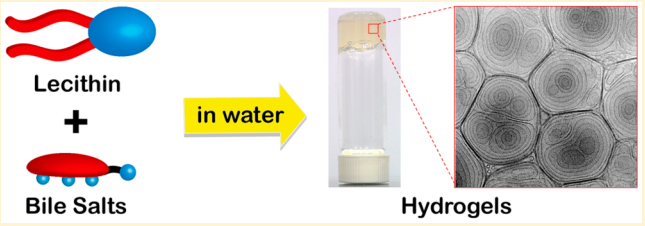

1. INTRODUCTION

Gels refer to materials with three-dimensional networks of gelators connected to each other by either chemical or physical bonds throughout a liquid. The gelators can be polymer, small organic molecules, or inorganic particles.[1] In general, the network in gels is permanent, meaning that the material will behave as a true solid and not relax with time even though gels are structurally disordered and may contain high volume fractions of liquid trapped within the networks. In contrast, a network of entangled long chains is a transient one, so that the corresponding fluid will be viscoelastic, not elastic, and will relax at long time scales. Gels are attractive to scientists and engineers not only because their structures are fascinating but also because they are among the most practical colloidal systems widely used in consumer, healthcare, and food products.[2,3]

In recent years, the molecular gels that are spontaneous assemblies of small molecules have drawn much attention in the chemical and biological sciences.[4,5] Various types of gelator molecules have been reported. Some are capable of gelling water (hydrogels),[4] and others can gel organic solvents (organogels).[5] While the network in gels often has a filamentous structure that connects at junction points, including chains, tubes, tapes, and fibers,[6−11] there has been a class of gels or gel-like materials formed by vesicles.[12] Vesicle are spherical containers with surrounded bilayer membranes self-assembled by amphiphilic molecules.[13] Vesicular gels have been found in some synthetic surfactant−cosurfactant−water systems, where the vesicles are closely packed to cause the solidlike behavior[14−21] or in gemini surfactant−water system that form networks of vesicle strings.[22] For the widely studied liposome systems (i.e., vesicles formed by biological lipids), gel or gel-like phases can only occur in highly concentrated solutions with crowded vesicles[12,23] or below the chain meting temperature where lipids are in crystalline states.[24] To the best of our knowledge, vesicular hydrogels formed completely by biomolecules at intermediate concentration have not been reported so far.

The synergistic assembly of two classes of biological amphiphiles, lecithin and bile salts (Figure 1), has continuously been an attractive topic in colloidal science.[12,25,26] Lecithin (i.e., phosphatidylcholine) is a type of zwitterionic amphiphile that is electrically neutral but has a positive charge on the choline group and a negative charge on the phosphate.[27] Bile salts are also physiological surfactants that bear unusual hydrophilic and hydrophobic faces. Since bile salts and lecithin are the main components involved in the physiological function of bile, much effort has been made to resolve the structures of the mixed micelles formed by bile salts and lecithin in water.[28−32] Most of the studies have focused on the dilute solutions where a structural transition from bilayer to cylindrical and then spheroidal micelle has been evidenced as the molar ratio of bile salt to lecithin increases.[33−41] Recently, we have reported that lecithin-bile salt mixed micelles in water can grow into long, flexible wormlike structures that exhibit viscoelastic behavior at a specific bile salt/lecithin molar ratio (near equimolar) and in the presence of a sufficient concentration of background electrolyte.[34] Apart from the aqueous solutions, lecithin in low polar solvents also show interesting self-assembly behaviors. Lecithin reverse spherical micelles can be induced to form

Received: September 1, 2015
Revised: November 2, 2015
Published: November 17, 2015

DOI: 10.1021/acs.langmuir.5b03267
Langmuir 2015, 31, 13312−13320

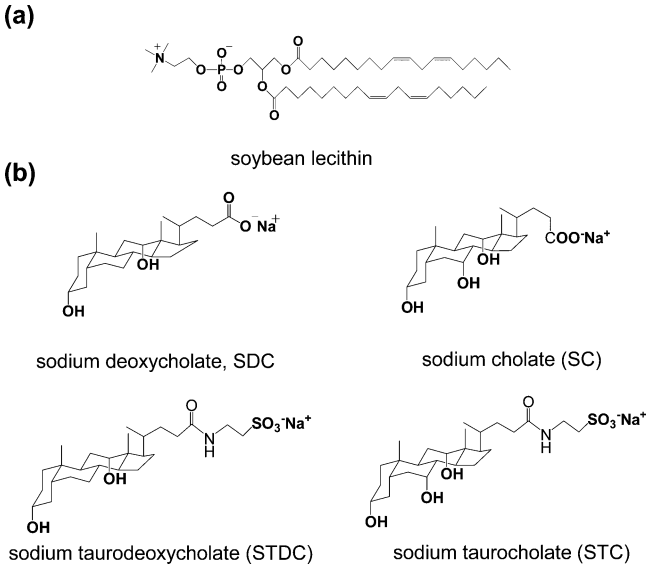

Figure 1. Molecular structures of (a) soybean lecithin and (b) bile salts used in this study.

wormlike micelles when mixed with bile salts, and as a result, the viscosity increases by more than 5 orders of magnitude.[42] Moreover, the addition of simple salts, such as $CaCl_2$, into lecithin organic solutions can even cause a solidlike behavior (i.e., formation of organogels).[43]

In this work, we focused on the lecithin-bile salt mixtures at intermediate concentration in water without the background electrolyte and found that at low bile salt/lecithin molar ratios where the bilayers have not been transformed into micelles, a stable gel phase can be formed at a lecithin concentration of 200 mM (~15 wt %) above the chain melting temperature of lecithin, which is much lower than the concentration of previous lecithin gels. Through the techniques of rheology, cryo-TEM, and scattering, we show that the solidlike property of the hydrogel is due to the formation of swollen multilamellar vesicles that impinge one another. The biological hydrogels can be obtained by incorporation of all the four different bile salts shown in Figure 1b in similar conditions. The gel is sensitive to ionic strength and when a small amount of inorganic salts, such as NaCl, is added, the gel is transformed into low-viscosity turbid liquids. Additionally, as the bile salt/lecithin molar ratio increases, a structural transition from multilamellar vesicles to cylindrical micelles and then to spheroidal micelles is observed, resulting in varying rheological properties of solutions, including gel, viscoelastic fluid, gel-like fluid, and low-viscous liquid in sequence. We will propose the mechanisms to explain why the hydrogel forms and why a series of structures can be obtained by tuning the bile salt/lecithin molar ratio.

The hydrogels formed by lecithin-bile salt mixtures are significant both from a science and application point of view. Scientifically, the findings in this work could be useful for understanding the interactions among lecithin, bile salts, and inorganic salts which are the main components in bile.[44,45] The nonallergic, biofriendly liposomes have been used as nanocarriers for delivering drugs.[46,47] The advantages of vesicular lipid hydrogels over conventional liposome solutions include their ability to increase the encapsulation efficiency through the multicompartment structure and the nearly immobile media that minimizes drug leakage during storage.[48−51] Furthermore, the tunable number of bilayers may serve as transport barriers for drugs to be released in a controlled manner. Along with the simple manufacturing processes, the biocompatible lecithin-bile salt hydrogels are promising as carriers for delivering active ingredients.

2. EXPERIMENTAL SECTION

2.1. Materials. Soybean lecithin (95% purity) was purchased from Avanti Polar Lipids, Inc. The bile salts, sodium deoxycholate (SDC, > 97% purity), sodium cholate (SC, > 99%), sodium taurocholate (STC, > 97%), and sodium taurodeoxycholate (STDC, > 95%) were purchased from Sigma-Aldrich. Sodium chloride (NaCl, > 99.7%) was purchased from J. T. Baker. All chemicals were used as received.

2.2. Sample Preparation. Lecithin and bile salts were first separately dissolved in methanol to prepare stock solutions (200 mM), and the molar ratios of bile salt to lecithin were tuned by mixing the stock solutions. Methanol was then removed by drying the samples in a vacuum oven at 50 °C for 48 h. The samples with varying concentrations were obtained by adding the deionized water, followed by stirring until the solutions become homogeneous.

2.3. Rheological Studies. We performed steady and dynamic rheological experiments on an AR2000EX stress-controlled rheometer (TA Instruments). Cone-and-plate geometry (40 mm diameter and 4° cone-angle) was used for all samples. The plate was equipped with Peltier-based temperature control, and all samples were studied at 25 ± 0.1 °C. We utilized a solvent trap to minimize evaporation of water. Dynamic frequency spectra were conducted in the linear viscoelastic regime, as determined from dynamic strain sweep measurements. For steady-shear experiments, sufficient time was allowed before data collection at each shear rate to ensure that the viscosity reached its steady-state value.

2.4. Small Angle X-ray and Neutron Scattering (SAXS and SANS). SAXS measurements were conducted on the BL23A1 beamline in the National Synchrotron Radiation Research Center (NSRRC), Taiwan.[52] A monochromatic beam of λ = 0.8 Å was used. All samples were studied at 25 °C. The scattering patterns were collected on a Pilatus 1M-F detector over a wave vector q range from 0.006 to 0.4 $Å^{-1}$. The spectra are shown as plots of the absolute intensity I versus wave vector $q = 4\pi \sin(\theta/2)/\lambda$, where θ is the scattering angle and λ is the wavelength. SANS measurements were made on Quokka beamline (40 m) at ANSTO in Sydney, Australia. Neutrons with a wavelength of 5 Å were selected. The q range was from 0.023 to 0.5 $Å^{-1}$.

2.5. SANS Modeling. Modeling of SANS data was conducted using the package provided by NIST with IGOR Pro.[53] For solutions of concentrated lamellae with d periodic spacing, such as multilamellar vesicles, the scattering intensity $I(q)$ can be modeled in terms of the form factor $P(q)$ and the structure factor $S(q)$ as follow[54,55]

$$I(q) = \frac{2\pi P(q)S(q)}{dq^2} \quad (1)$$

The form factor for lamella of thickness δ, variation in lamella thickness σ, and excess scattering length density $\Delta\rho$ is given by

$$P(q) = \frac{2\Delta\rho^2}{q^2}[1-\cos(q\delta)e^{-q^2\sigma^2/2}] \quad (2)$$

The structure factor for the lamellar stacks can be described as

DOI: 10.1021/acs.langmuir.5b03267
Langmuir 2015, 31, 13312−13320

$$S(q) = 1 + 2\sum_{1}^{N-1}\left(1 - \frac{n}{N}\right)\cos\left(\frac{qdn}{1 + 2\Delta q^2 d^2 \alpha(n)}\right) \times \exp\left(-\frac{2q^2 d^2 \alpha(n) + \Delta q^2 d^2 n^2}{2(1 + 2\Delta q^2 d^2 \alpha(n))}\right)\frac{1}{\sqrt{1 + 2\Delta q^2 d^2 \alpha(n)}} \quad (3)$$

where N is the number of lamellar plates, Δq is instrumental resolution, and $\alpha(n)$ is given by

$$\alpha(n) = \frac{\eta_{cp}}{4\pi^2}[\ln(\pi n) + \gamma_E] \quad (4)$$

γ_E is Euler's constant, equal to 0.5772156649, and η_{cp} is the Caillé parameter that measures the bilayer fluctuations given by

$$\eta_{cp} = \frac{q_0^2 k_B T}{8\pi\sqrt{K\bar{B}}} \quad (5)$$

where K is the smectic bending elasticity, q_0 is the value of first-order Bragg peak, k_B is the Boltzmann's constant, T is temperature, and $\bar{B}$ is the compression modulus.

2.6. Cryogenic Transmission Electron Microscopy (cryo-TEM). Specimens for cryo-TEM were prepared with a FEI Vitrobot Mark IV vitrification system at 22 °C and 100% relative humidity. Samples were transferred onto grids with carbon films, and an appropriate blotting process was applied. The grids were immediately plunged into liquid ethane after blotting and then stored in liquid nitrogen before imaging. Cryo-TEM experiments were conducted on a FEI Tecnai G2 transmission electron microscope operated at a voltage of 120 kV. Low-dose mode was used to minimize radiation damage of samples.[56] The tomographic image was reconstructed with 3DXplorer provided by FEI Company and then modeled with Amira.[57]

2.7. Zeta Potential. The measurement of zeta potential was carried out on a Brookhaven 90 Plus light-scattering instrument, which measures the electrophoretic mobility of the particles in an electrical field, and a Helmholtz-Smoluchowski equation was used to convert the electrophoretic mobility into zeta potential.[58,59] Samples with lower concentrations (<100 mM) were prepared and were sonicated for 72 h before measurement.

3. RESULTS AND DISCUSSION

3.1. Phase Behavior and Rheological Property. We first discuss the phase behaviors of lecithin-bile salt mixtures in aqueous solution, and the samples at lecithin concentration of 400 mM (~25 wt %) mixed with varying amount of SDC are taken as examples. Figure 2 shows the phases and the corresponding zero-shear viscosity η_0 of the samples as a function of B_0, the molar ratio of bile salt to lecithin. The phases of the mixtures are sensitively dependent on B_0, and five distinct regimes are observed. The solubility of lecithin in water is limited due to the two bulky hydrophobic tails, and lecithin alone (i.e., $B_0 = 0$) tends to form bilayers in water. The pure lecithin solution is turbid, and the viscosity is only slightly higher than that of pure water. Surprisingly, when lecithin is mixed with a small amount of bile salt, $0.1 < B_0 < 0.3$, the solutions transform into nonflow ones (i.e., solidlike gels). The gels are bluish and translucent, a manifestation of the Tyndall effect that is indicative of the presence of vesicles.[60] The solutions can hold their own weight in an inverted vial as shown in the photograph of Figure 2. The zero-shear viscosity in this regime is infinite, and the representative dynamic rheological data of the mixture with $B_0 = 0.2$ are shown in Figure 3a, where the elastic modulus (G') is nearly independent of frequency (ω) and is larger than the viscous modulus (G'') in the whole range of frequency, which is typical of gels. In addition to SDC, the other three bile salts, including SC, STDC, and STC (Figure 1), all behave similarly in this B_0

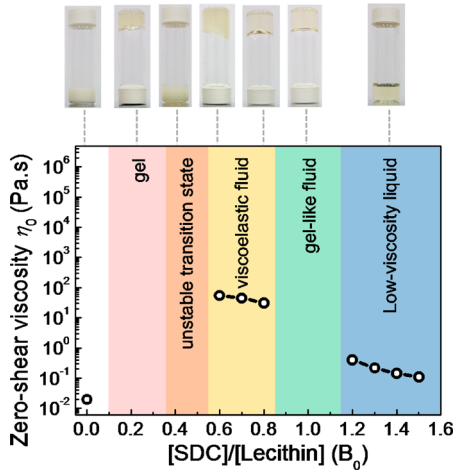

Figure 2. Phase behaviors of lecithin-SDC mixtures in water and zero-shear viscosity as a function of SDC/lecithin molar ratio B_0 for viscoelastic fluids and low-viscosity liquids. The lecithin concentration is fixed at 400 mM.

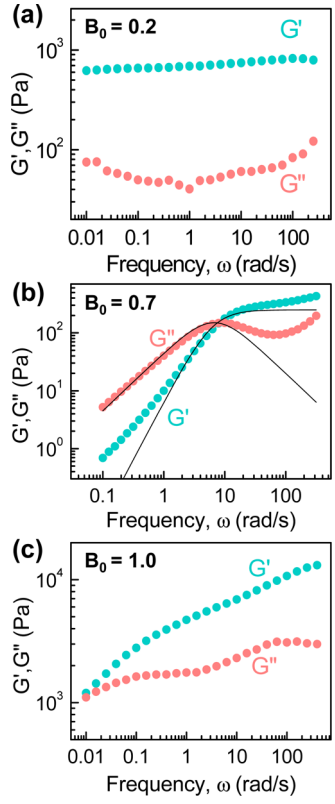

Figure 3. Dynamic rheology of lecithin-SDC mixtures in (a) gel phase at B_0 = 0.2, (b) viscoelastic phase at B_0 = 0.7, and (c) gel-like phase at B_0 = 1.0. The concentration of lecithin is fixed at 400 mM. The solid curves in (b) are the fits of single-relaxation-time Maxwell model.

DOI: 10.1021/acs.langmuir.5b03267
Langmuir 2015, 31, 13312−13320

range. The dynamic rheological data of the gels induced by SC, STDC, and STC at B_0 = 0.2 are shown in Figure S1.

At B_0 > 0.3, the solutions become white and opaque again. Simultaneously, the solidlike behavior disappears and the solutions start to flow with a sudden drop of viscosity beyond a very weak yield stress. An unstable phase transition with a large fluctuation of concentration should occur in this region. As B_0 increases to 0.6, the solution remains cloudy, but it forms a stable high-viscosity fluid that flows slowly in an inverted vial. The solution gradually turns to be transparent with increasing B_0, as shown by the representative photograph of the sample at B_0 = 0.8 in Figure 2. The dynamic rheological data of the mixture at B_0 = 0.7 is shown in Figure 3b. A crossover of G' and G'' that separates the solidlike region ($G' > G''$) at high frequency and the liquid-like region ($G'' > G'$) at low frequency indicates a viscoelastic behavior, and the data can be approximately described by the singe-relaxation-time Maxwell model shown as the solid curves.[34,42] In surfactant solutions, such a viscoelastic behavior is generally caused by entangled wormlike micelles.[34,42] At B_0 between 0.9 and 1.1, the mixtures form a transparent phase with a viscosity so high that the solutions are nearly immobile in an inverted vial. The dynamic data at B_0 = 1.0 shown in Figure 3c reveal that although moduli are frequency-dependent, G' and G'' cross each other at a very low frequency (below 0.01 rad/s), indicating that the relaxation time of the long micelles are so large that the solution behaves like a gel in a practical time scale.[43] Further enhancing B_0 to above 1.2 leads to a sharp decrease in the viscosity, and the solutions are all transparent. The long cylindrical micelles are transformed into short or even spherical ones as bile salts become the major component in the mixtures.[33,34]

The gel phase can be formed at lecithin concentration as low as 200 mM (~15 wt %) with B_0 between 0.1 and 0.3. Below 200 mM, the solutions are low-viscosity liquids in the whole range of B_0. The dynamic rheology data of the gel samples composed of 200 and 300 mM lecithin at B_0 = 0.2 are shown in Figure S2. The stability of the gels is concentration-dependent. The gels formed at lecithin concentration higher than 250 mM can remain stable for more than one year and show excellent thermal durability even close to the boiling point of water (Figure S3), while those formed around 200 mM only stand for about a month before transforming into low-viscosity solutions. The stability of the gels is also affected by additional electrolytes. When 100 mM sodium chloride (NaCl) is added to the gel of 300 mM lecithin, the sample turns to be an opaque liquid with a low viscosity ~0.03 Pa s. The effect of pH on the gel is shown in Figure S4. The rheological property of the gel is not significantly affected by pH value in the range between 5 and 9, indicating the gel is not sensitive to pH values. At pH = 2 and 12, however, the elastic modulus of the gel decreases, which could be due to the degradation of lecithin in a strong acidic and basic environment. Moreover, it is noticed that the transparent gel-like phase formed at B_0 around 1.0 only appears in the solutions with a lecithin concentration higher than 400 mM, implying the high relaxation time found in Figure 3c originates from crowded long micelles.

3.2. Cryogenic Transmission Electron Microscopy (cryo-TEM). The lecithin-bile salt (SDC) mixtures in water were investigated by cryo-TEM to correlate the self-assembled structures to the rheological properties. The samples for cryo-TEM were rapidly frozen into a solid amorphous state so that the original structures in solutions were preserved. Figure 4a shows the cryo-TEM image of pure lecithin (B_0 = 0) at 300 mM where a stack of undulated lamellae (bilayers) can be seen. The large aggregates of the bilayers are the origin of the sample turbidity shown in Figure 2. The image of the gel sample at a 300 mM lecithin concentration with B_0 = 0.2 is shown in Figure 4b. The sample fills up with multilamellar vesicles that strongly impinge on one another, even creating planar boundaries. Notably, in comparison with the closely packed lamellae of pure lecithin (Figure 4a), the spacing between the lamellae in the gel is much larger. It is apparent that the solid-like behavior of the gel arises from the jammed swollen multilamellar vesicles that hinder the solution to flow. Also, because of the swelling of the lamellae, the sample turns to be translucent (Figure 2). We further utilized the tomography technique to reconstruct the three-dimensional (3D) structure in the gel, as shown in Figure 4c, which confirms that the lamellae repel one another and swell to fill the whole space. The cryo-TEM image of the gel formed at 200 mM lecithin concentration (B_0 = 0.2) is shown in Figure S5a where similar jammed multilamellar vesicles can be seen, but the collision is not as hard as those at 300 mM due to the lower concentration.

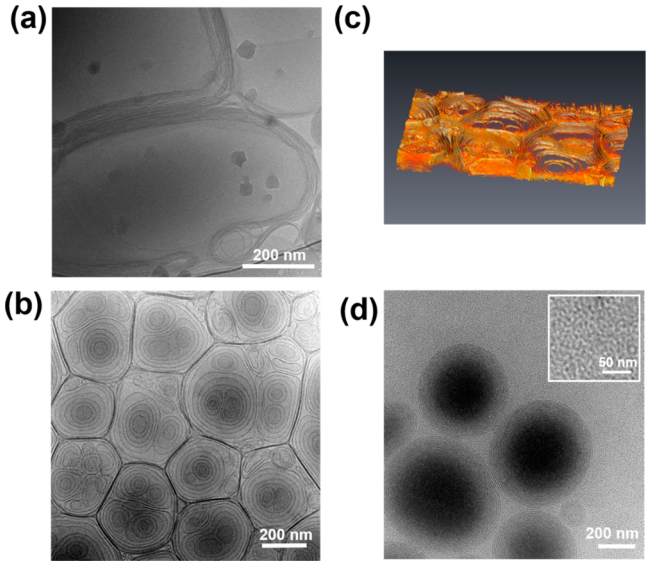

Figure 4. Cryo-TEM images of (a) pure lecithin, (b) gel formed by lecithin-SDC mixture at B_0 = 0.2, (c) 3D tomography image of the gel at B_0 = 0.2, and (d) viscoelastic solution at B_0 = 0.7. The lecithin concentration is 300 mM.

Figure 4d shows the cryo-TEM image of the cloudy and viscoelastic sample at 300 mM lecithin concentration and B_0 = 0.7 (Figure 2). Different from the structure in gels, the viscoelastic fluid comprises a coexistence of large multilamellar vesicles and wormlike micelles. The inset is the enlarged image of the curly wormlike micelles that bring about the viscoelasticity of the sample. The presence of the multilamellar vesicles should be responsible for the deviation of the dynamic rheology from the Maxwell model that generally shows good fit to pure wormlike micellar solutions (Figure 3b). Note that the *d*-spacing of the lamellae in the vesicles here greatly shrinks, and the lamellae closely stack as those of pure lecithin but in a more regular fashion. The cloudiness is attributed to the strong light scattering of these stacked lamellae.

As described in the preceding section, the gel phase only exists at a lecithin concentration above 200 mM and in a narrow B_0 range between 0.1 and 0.3. The cryo-TEM image of the sample at a lower lecithin concentration of 150 mM with B_0

DOI: 10.1021/acs.langmuir.5b03267
Langmuir 2015, 31, 13312−13320

= 0.2 is shown in Figure 5a. The sample is low viscous and turbid, and as the image reveals, it contains a great number of

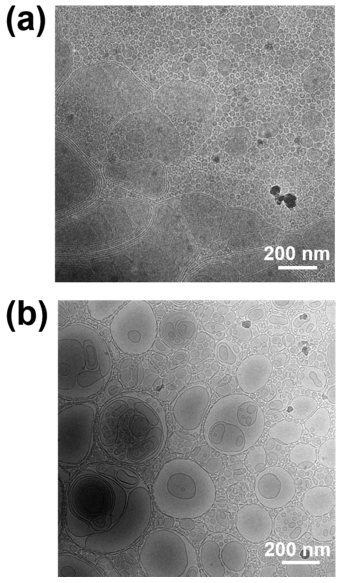

Figure 5. Cryo-TEM images of low-viscosity solutions formed by lecithin-SDC mixtures: (a) at a low lecithin concentration of 150 mM and B_0 = 0.2, and (b) with the addition of 100 mM NaCl into the sample at lecithin concentration 300 mM and B_0 = 0.2 that is originally a gel.

isolated small unilamellar vesicles along with large multilamellar ones. The concentration below 200 mM is too low for the vesicles to interlock one another. Figure 5b shows the cryo-TEM image of the original gel sample (300 mM lecithin concentration and B_0 = 0.2) with the addition of 100 mM NaCl. It can be seen that most of the jammed multilamellar vesicles are transformed into isolated unilamellar ones, which explains the disappearance of solidlike behavior and the transition to a low-viscosity liquid in the presence of additional electrolytes. Similar unilamellar vesicles can be seen after the addition of 100 mM NaCl into the gel sample at 200 mM lecithin concentration and B_0 = 0.2, as shown in the cryo-TEM image of Figure S5b.

3.3. Small Angle X-ray and Neutron Scattering (SAXS and SANS). In addition to cryo-TEM that only takes local images, we utilized SAXS and SANS to probe the self-assembled structures in the lecithin-bile salt (SDC) mixtures. The SAXS data of the mixtures at 400 mM lecithin concentration with varying B_0 are shown in Figure 6, which can be directly compared to the phases in Figure 2. Pure lecithin (B_0 = 0) in water shows diffraction peaks with q values in 1:2 ratio, typical of the lamellar structure, and the d-spacing is 6.47 nm. At B_0 = 0.1 where only a small amount of bile salt is added, the peaks remain in a 1:2:3 ratio, but drastically downshift to q values corresponding to a much larger d-spacing of 13.59 nm, indicative of a prominent swelling of the lamellae. Although the diffraction data all reveal lamellar structure at B_0 between 0.1 and 0.8, some subtle changes can be found to support the cryo-TEM images and the rheological properties. In the gel phase region with swollen lamellae (B_0 = 0.1−0.3), the diffraction peaks are broader, reflecting a less regular arrangement of the bilayers in gels as shown in Figure 4b. As B_0 exceeds the phase boundary of gels to 0.4, much sharper peaks that suddenly shift to higher q are observed. The q value of the

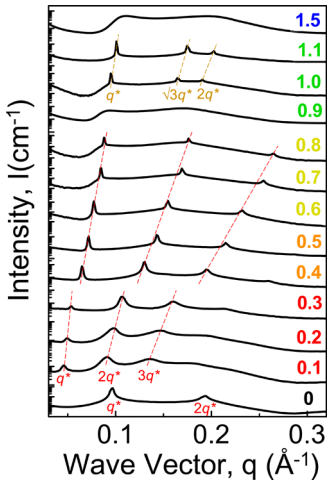

Figure 6. SAXS data of lecithin-SDC mixtures with varying B_0 at a fixed lecithin concentration of 400 mM.

peaks then gradually increases with increasing B_0 until 0.8. This implies more ordered and closer-packed lamellae in vesicles are formed above B_0 = 0.4, consistent with the cryo-TEM image of the sample at B_0 = 0.7 shown in Figure 4d where the d-spacing of the multilamellar vesicles shrinks to 7.45 nm. The shift of the diffraction peaks to higher q as B_0 increases results from the combination of two aspects: the increase of total lipid concentration and the screening of electrostatic repulsive forces between bilayers. The latter should be the primary cause, which will be discussed in the Mechanism section. Note that at B_0 between 0.4 and 0.8, as shown in Figure 2, a phase transition region appears first, followed by a viscoelastic fluid as B_0 increases. Although there are structures other than bilayers that coexist with multilamellar vesicles in this region, such as wormlike micelles, only the vesicles that contain periodical structure produce distinct diffraction peaks.

At B_0 = 0.9, all the diffraction peaks disappear, implying a complete transformation of the multilamellar vesicles into disordered long cylindrical micelles. It is interesting that at B_0 = 1.0 and 1.1, the diffraction peaks appear again and the q values are in a ratio of 1:$\sqrt{3}$:2, which generally infers a hexagonal pack of cylinders. The gel-like behavior of the solutions is thus suggested to be caused by the closely packed long cylindrical micelles. The sample at B_0 = 1.0 shows strong birefringence between crossed polarizers as shown in Figure S6, further confirming this argument. At B_0 = 1.5, the diffraction peaks vanish again. Along with the evidence from the sharply decreased viscosity and the transparent appearance, it is rational to conclude that disordered short micelles are formed at such a high B_0. The SAXS data obtained at a 300 mM lecithin concentration with varying B_0 are shown in Figure S7. The dependence of the structure on B_0 is essentially the same as that at 400 mM, except that the cylindrical micelles are not forced to pack hexagonally at B_0 around 1.0 due to the lower concentration that is unable to create a lyotropic-ordered phase.

In addition to SAXS, the gel samples of 200 and 300 mM lecithin concentration at B_0 = 0.2 were further investigated by SANS. Instead of protonated water, the samples for SANS were prepared in deuterated water. The data are shown in Figure 7 and the intensity versus q curves are unlike the SAXS data shown in Figure 6 due to the different scattering mechanism. X-ray scattering originates from the contrast of the electron density in three distinct domains in the present case, including

DOI: 10.1021/acs.langmuir.5b03267
Langmuir 2015, 31, 13312−13320

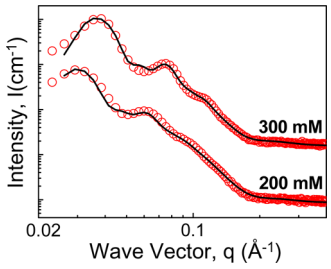

Figure 7. SANS data of the gels formed by lecithin-SDC mixtures at 200 and 300 mM lecithin concentration, repectively. The B_0 is fixed at 0.2 for both samples. Model fits are shown as the solid lines through the data.

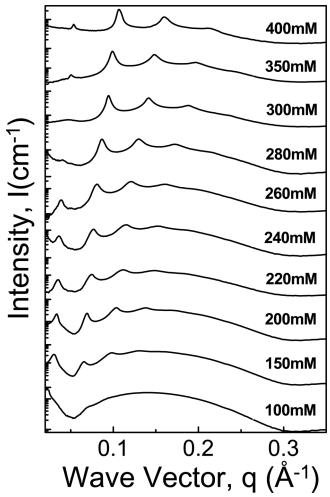

Figure 8. SAXS data of lecithin-SDC mixtures at different lecithin concentrations with B_0 at 0.3.

water, exterior hydrophilic regions, and interior hydrophobic regions of the bilayers, while only two domains (i.e., deuterated water and protonated bilayers are distinguishable for neutron scattering). One advantage of SANS experiments is that the structural information on the bilayers can be extracted by analyzing the relatively uncomplicated form factor of the SANS data. We used the multilamellar model (eqs 1−5) to fit the SANS data as the solid curves shown in Figure 7. The SANS data can be well fit by the model, and the fitting parameters are listed in Table 1. The bilayer thickness is around 3 nm and the *d*-spacings of the gels at 200 and 300 mM lecithin concentration are 19.58 and 16.12 nm, respectively, consistent with the cryo-TEM images shown in Figure 4b and Figure S5a. The increase in the number of bilayers with increasing concentration from the fitting agrees with the cryo-TEM images as well.

The effect of the concentration on the structure was also studied by scattering. The SAXS data of pure lecithin in water at varying concentration are shown in Figure S8. For pure lecithin that form stacked bilayers in water, the diffraction peaks are all sharp and the *d*-spacing is fixed at ∼6.4 nm from 100 to 400 mM, indicating the thickness of the wetting layer between lamellae is independent of lecithin concentration. Figure 8 shows the SAXS data of lecithin-bile salt (SDC) mixtures at B_0 = 0.3 in water at different lecithin concentrations. At 100 mM, no diffraction peak is found, confirming the formation of isolated unilamellar vesicles at low concentration that are unable to gel the solution. When the lecithin concentration is higher than 150 mM, broad diffraction peaks from swollen multilamellar vesicles appear and the peaks intensify with increasing concentration. Furthermore, the *d*-spacing of the multilamellar vesicles reduces as the concentration increases, in contrast to the constant *d*-spacing of pure lecithin. Along with the cryo-TEM image and the rheological data, it is apparent that above 200 mM, the swollen multilamellar vesicles are capable of filling the whole space so that an increase of concentration inevitably suppresses the distance between bilayers so as to accommodate more bilayers. Note that the intensity of the first-order peak is weaker than that of the high-order ones at the concentration above 260 mM and nearly disappears at 300 mM, which is because the first-order peak happens to be around the *q* where the form factor of the bilayer is at its minimum.

3.4. Mechanism. It is well-known that the self-assembled structures of amphiphiles in solutions are governed by the critical packing parameter (CPP) of the molecule (i.e., the ratio of the effective tail area to headgroup area).[13] Because of the bulky tails, lecithin alone in water has a CPP ∼ 1 and tends to organize into bilayers, which, however, are generally in the form of large stacks if no vigorous external force is applied due to the low stability of lecithin in water. Bile salts are anionic amphiphilic molecules, and the solubility of bile salts in water is much higher than that of lecithin.[61] Previous studies have shown that bile salts prefer to bind the headgroups of lecithin in water. The addition of bile salts into lecithin aqueous solutions have two major effects. First, the insertion of bile salts expands the headgroup area more than the tail area of lecithin, thus leading to a decrease of effective CPP. Second, the negatively charged groups on bile salts that bring about repulsion in water can greatly enhance the stability of the mixed aggregates.[62] It has been found that in dilute aqueous solutions, as the ratio of bile salts increases, the self-assembled structure of lecithin-bile salt mixtures transforms from stable unilamellar vesicles to cylindrical micelles, and then to small spheroidal micelles due to the gradual decrease of CPP.[37] This can explain the similar structural evolution in the present system with increasing B_0. The formation of the gel phase at B_0 between 0.1 and 0.3, however, is unusual.

The cryo-TEM images have clearly shown that the solidlike behavior of the gel phases is caused by the space-filling swollen multilamellar vesicles (Figure 4b). The dramatic increase of the bilayer *d*-spacing have to do with the increasing repulsive forces between bilayers. Thus, the change of the surface charges on the bilayers with B_0 must play an important role in the structural transition. To verify this point, we employed the electrokinetic measurements to obtain the electrostatic potential near the charged surface (i.e., zeta potential). Since

Table 1. Fitting Parameters of SANS Data Shown in Figure 7 from Modeling

[lecithin] (mM)	bilayer spacing *d* (nm)	bilayer thickness δ (nm)	polydispersity of thickness σ	no. of lamellar plate *N*	Caillé parameter η_{cp}
200	19.58 ± 0.017	3.09 ± 0.190	0.22 ± 0.01	3	0.27 ± 0.004
300	16.12 ± 0.014	3.22 ± 0.017	0.21 ± 0.01	4	0.20 ± 0.002

DOI: 10.1021/acs.langmuir.5b03267
Langmuir 2015, 31, 13312−13320

the gel samples are not suitable for the electrokinetic experiments, we only measured the zeta potentials for the samples at lecithin concentrations below 100 mM. Although the data may not be able to exactly quantify the zeta potential at high concentration, they can be used to qualitatively explain the varying repulsive force between bilayers.

Figure 9 shows the zeta potentials of the lecithin-bile salt (SDC) mixtures as a function of B_0 at lecithin concentration of

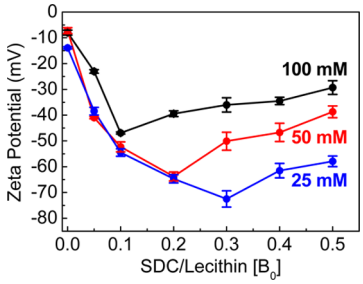

Figure 9. Zeta potential as a function of B_0 for lecithin-SDC mixtures at lecithin concentrations of 25, 50, and 100 mM.

25, 50, and 100 mM. For all three lecithin concentrations, the zeta potential initially becomes more negative with increasing B_0, which is due to the incorporation of negatively charged bile salt molecules into the bilayers. After reaching the minimum, however, the zeta potential turns to be less negative when more bile salts are added. As the amount of bile salts in the bilayers exceeds a threshold, the contribution of the electrostatic attractive energy to the free energy dominates over the contribution from the translational entropy of free counterions. Thus, the counterions (Na^+) prefer to condense on the surface to lower the free energy instead of staying free in the solutions.[63] The increasing number of condensed counterions therefore more effectively screens the electrostatic repulsion as B_0 increases. Note that the B_0 for the most negative zeta potential (B_0^{min}) is concentration-dependent, changing from 0.3 to 0.1 as the lecithin concentration increases from 25 to 100 mM. It has been shown that there is an approximately constant concentration of free bile salts dissolving in water in equilibrium with the bile salts in bilayers.[33] In other words, at the same B_0, the amount of bile salts that incorporate into the bilayers is less for the sample with a lower lecithin concentration. A higher B_0 is thus required for the lower-concentration mixtures to reach the most negative zeta potential.

Figure 9 provides important information for elucidating the mechanism of the gel formation. When a small amount of bile salts are incorporated into lecithin bilayers (i.e., $B_0 = 0.1-0.3$), the negatively charged bile salts cause a strong repulsive force between bilayers. The bilayers thus greatly swell and prefer to form smaller-scaled unilamellar vesicles if the space is sufficiently large to allow the translational entropy of the vesicles to increase. This is the phenomenon observed at a lecithin concentration below 200 mM (Figure 5a), where the isolated unilamellar, however, is unable to significantly enhance the viscosity. When the lecithin concentration is higher than 200 mM, because of the limited space, the highly swollen multilamellar vesicles impinge first and reach a force balance before transforming into small unilamellar vesicles (Figure 4b). It is known that the dynamic exchange processes of lipid bilayers in water are very slow due to the low solubility of the lipids.[64,65] Therefore, the interlocked multilamellar vesicles form a sturdy network that holds the solutions and imparts the solidlike behavior. Note that multilamellar vesicles are generally not in a thermodynamically stable state,[66] which explains why the gel formed at low lecithin concentration (200 mM) can last only for one month. The electrostatically repelled bilayers can be destabilized by the addition of extra electrolytes that screen the strong repulsive interactions and reduces the distance between bilayers, thus sparing room to facilitate the formation of unilamellar vesicles. This is why the elastic behavior disappears as NaCl is added into gels (Figure 5b).

When B_0 exceeds the boundary of the gel phase, the sample immediately turns to be opaque, similar to the pure lecithin sample, which is ascribed to the shrinkage of d-spacing in multilamellar vesicles. The decrease of d-spacing is evidenced by SAXS data shown in Figure 6 and can be explained by the weakening of the repulsive force at B_0 higher than B_0^{min} as shown in Figure 9. The more closely stacked bilayers widen the disparity of the refractive index between the vesicles and water, which, along with the large size of the vesicles, is responsible for the strong light scattering that causes the opaqueness. In the transition region, the multilamellar vesicles with a short d-spacing is accompanied by the cylindrical micelles that evolve from part of the vesicles due to the decrease of the CPP upon the insertion of bile salts (Figure 4d). The vesicles completely turn to be cylindrical micelles, followed by the transformation into even smaller spheroidal micelles as more bile salts are incorporated to further reduce CPP.

4. CONCLUSIONS

We have shown lecithin-bile salt mixtures in water at intermediate to high concentration can self-assemble into a variety of structures that lead to rich rheological properties, including solid-like gels and viscoelastic fluids, depending on the bile salt/lecithin molar ratio. The most intriguing one among all the structures is the gel formed by swollen multilamellar vesicles, which is suggested to be caused by the electrostatic repulsion of surface charges brought by bile salts. This work makes progress in clarifying the role of bile salts in the physiological processes involving lecithin and bile salt. In comparison with other lipid gel systems, the one presented in this study can be formed at a relatively low concentration and shows good long-term and thermal stability. Furthermore, such vesicular gels provide multicompartment reservoirs for drug encapsulation that may allow a slow and controllable release of the drugs. The hydrogel is formed completely by abundant biomolecules, and thus the biocompatible, low-cost gel is high potential for cosmetic and medical applications.

■ ASSOCIATED CONTENT

Supporting Information

The Supporting Information is available free of charge on the ACS Publications website at DOI: 10.1021/acs.langmuir.5b03267.

Dynamic rheology, cryo-TEM images, birefringence photograph, and SAXS data (PDF)

■ AUTHOR INFORMATION

Corresponding Author

*E-mail: shtung@ntu.edu.tw.

Notes

The authors declare no competing financial interest.

DOI: 10.1021/acs.langmuir.5b03267
Langmuir 2015, 31, 13312−13320

■ ACKNOWLEDGMENTS

This work was financially supported by the grant of the Ministry of Science and Technology, Taiwan (103-2221-E-002-186-MY3). We acknowledge NSRRC, Taiwan, for facilitating the SAXS experiments and for sponsoring the travel expense of SANS experiments. The assistance in scattering experiments from Dr. U-Ser Jeng of NSRRC and Drs. Jitendra Mata and Chris Garvey of ANSTO are also acknowledged.

■ REFERENCES

(1) Sangeetha, N. M.; Maitra, U. Supramolecular gels: functions and uses. *Chem. Soc. Rev.* **2005**, *34*, 821−836.
(2) Zhang, J.; Yan, J.; Pageni, P.; Yan, Y.; Wirth, A.; Chen, Y.-P.; Qiao, Y.; Wang, Q.; Decho, A. W.; Tang, C. Anion-responsive metallopolymer hydrogels for healthcare applications. *Sci. Rep.* **2015**, *5*, 11914.
(3) Banerjee, S.; Bhattacharya, S. Food gels: gelling process and new applications. *Crit. Rev. Food Sci. Nutr.* **2012**, *52*, 334−346.
(4) Estroff, L. A.; Hamilton, A. D. Water gelation by small organic molecules. *Chem. Rev.* **2004**, *104*, 1201−1218.
(5) Terech, P.; Weiss, R. G. Low molecular mass gelators of organic liquids and the properties of their gels. *Chem. Rev.* **1997**, *97*, 3133−3160.
(6) Osada, Y.; Gong, J.-P. Soft and wet materials: polymer gels. *Adv. Mater.* **1998**, *10*, 827−837.
(7) Munialo, C. D.; Martin, A. H.; van der Linden, E.; de Jongh, H. H. J. Fibril formation from pea protein and subsequent gel formation. *J. Agric. Food Chem.* **2014**, *62*, 2418−2427.
(8) van Herpt, J. T.; Stuart, M. C. A.; Browne, W. R.; Feringa, B. L. Mechanically induced gel formation. *Langmuir* **2013**, *29*, 8763−8767.
(9) Ichinose, W.; Miyagawa, M.; Yamaguchi, M. Reversible shrinkage of self-assembled two-component organogels by lithium salts: synthesis of gelation property and lithium salt response using bidomain helicene oligomer. *Chem. Mater.* **2013**, *25*, 4036−4043.
(10) Ye, F.; Chen, S.; Tang, G.; Ma, M.; Wang, X. Self-assembled nanofibrillar gel network toughened PMMA nanocomposite by in situ thermal polymerization of MMA gel. *Colloids Surf., A* **2015**, *480*, 1−10.
(11) Aggeli, A.; Bell, M.; Boden, N.; Keen, J. N.; Knowles, P. F.; McLeish, T. C. B.; Pitkeathly, M.; Radford, S. E. Responsive gels formed by the spontaneous self-assembly of peptides into polymeric [beta]-sheet tapes. *Nature* **1997**, *386*, 259−262.
(12) Elnaggar, Y. S. R.; El-Refaie, W. M.; El-Massik, M. A.; Abdallah, O. Y. Lecithin-based nanostructured gels for skin delivery: an update on state of art and recent applications. *J. Controlled Release* **2014**, *180*, 10−24.
(13) Israelachvili, J. N. *Intermolecular and Surface Forces*; Academic Press: San Diego, 2011.
(14) Grewe, F.; Ortmeyer, J.; Haase, R.; Schmidt, C. Colloidal Gels Formed by Dilute Aqueous Dispersions of Surfactant and Fatty Alcohol. In *Colloid Process Engineering*; Kind, M., Peukert, W., Rehage, H., Schuchmann, H. P., Eds.; Springer International Publishing: Switzerland, 2015, pp 21−43.
(15) Gradzielski, M.; Bergmeier, M.; Müller, M.; Hoffmann, H. Novel gel phase: a cubic phase of densely packed monodisperse, unilamellar vesicles. *J. Phys. Chem. B* **1997**, *101*, 1719−1722.
(16) Long, P.; Hao, J. A gel state from densely packed multilamellar vesicles in the crystalline state. *Soft Matter* **2010**, *6*, 4350−4356.
(17) Goetz, R. J.; El-Aasser, M. S. Dilute phase behavior of cetyl alcohol, sodium lauryl sulfate, and water. *Langmuir* **1990**, *6*, 132−136.
(18) Gradzielski, M. The rheology of vesicle and disk systems — relations between macroscopic behaviour and microstructure. *Curr. Opin. Colloid Interface Sci.* **2011**, *16*, 13−17.
(19) Gradzielski, M. Vesicles and vesicle gels—structure and dynamics of formation. *J. Phys.: Condens. Matter* **2003**, *15*, R655−R697.
(20) Abdel-Rahem, R.; Hoffmann, H. The distinction of viscoelastic phases from entangled wormlike micelles and of densely packed multilamellar vesicles on the basis of rheological measurements. *Rheol. Acta* **2006**, *45*, 781−792.
(21) Hoffmann, H.; Thunig, C.; Schmiedel, P.; Munkert, U. Surfactant systems with charged multilamellar vesicles and their rheological properties. *Langmuir* **1994**, *10*, 3972−3981.
(22) Menger, F. M.; Peresypkin, A. V. Strings of vesicles: flow behavior in an unusual type of aqueous gel. *J. Am. Chem. Soc.* **2003**, *125*, 5340−5345.
(23) Brandl, M.; Drechsler, M.; Bachmann, D.; Tardi, C.; Schmidtgen, M.; Bauer, K.-H. Preparation and characterization of semi-solid phospholipid dispersions and dilutions thereof. *Int. J. Pharm.* **1998**, *170*, 187−199.
(24) Shinto, K.; Hoffmann, H.; Watanabe, K.; Teshigawara, T. Hydrogels from diacylphosphatidylcholine. *Colloid Polym. Sci.* **2012**, *290*, 91−95.
(25) Hjelm, R. P.; Alkan, M. H.; Thiyagarajan, P. Small-angle neutron scattering studies of mixed bile salt-lecithin colloids. *Mol. Cryst. Liq. Cryst. Incorporating Nonlinear Opt.* **1990**, *180*, 155−164.
(26) Hjelm, R. P.; Thiyagarajan, P.; Alkan-Onyuksel, H. Organization of phosphatidylcholine and bile salt in rodlike mixed micelles. *J. Phys. Chem.* **1992**, *96*, 8653−8661.
(27) Hauser, H.; Phillips, M. C.; Levine, B. A.; Williams, R. J. P. Conformation of the lecithin polar group in charged vesicles. *Nature* **1976**, *261*, 390−394.
(28) Nichols, J. W.; Ozarowski, J. Sizing of lecithin-bile salt mixed micelles by size-exclusion high-performance liquid chromatography. *Biochemistry* **1990**, *29*, 4600−4606.
(29) Müller, K. Structural aspects of bile salt-lecithin mixed micelles. *Hepatology* **1984**, *4*, 134S−137S.
(30) Zimmerer, R. O.; Lindenbaum, S. Enthalpy of bile salt-lecithin mixed micelle formation. *J. Pharm. Sci.* **1979**, *68*, 581−585.
(31) Claffey, W. J.; Holzbach, R. T. Dimorphism in bile salt/lecithin mixed micelles. *Biochemistry* **1981**, *20*, 415−418.
(32) Nawroth, T.; Buch, P.; Buch, K.; Langguth, P.; Schweins, R. Liposome formation from bile salt−lipid micelles in the digestion and drug delivery model fassifmod estimated by combined time-resolved neutron and dynamic light scattering. *Mol. Pharmaceutics* **2011**, *8*, 2162−2172.
(33) Madenci, D.; Salonen, A.; Schurtenberger, P.; Pedersen, J. S.; Egelhaaf, S. U. Simple model for the growth behaviour of mixed lecithin-bile salt micelles. *Phys. Chem. Chem. Phys.* **2011**, *13*, 3171−3178.
(34) Cheng, C.-Y.; Oh, H.; Wang, T.-Y.; Raghavan, S. R.; Tung, S.-H. Mixtures of lecithin and bile salt can form highly viscous wormlike micellar solutions in water. *Langmuir* **2014**, *30*, 10221−10230.
(35) Meyuhas, D.; Bor, A.; Pinchuk, I.; Kaplun, A.; Talmon, Y.; Kozlov, M. M.; Lichtenberg, D. Effect of ionic strength on the self-assembly in mixtures of phosphatidylcholine and sodium cholate. *J. Colloid Interface Sci.* **1997**, *188*, 351−362.
(36) Egelhaaf, S. U.; Schurtenberger, P. Shape transformations in the lecithin-bile salt system: from cylinders to vesicles. *J. Phys. Chem.* **1994**, *98*, 8560−8573.
(37) Walter, A.; Vinson, P. K.; Kaplun, A.; Talmon, Y. Intermediate structures in the cholate-phosphatidylcholine vesicle-micelle transition. *Biophys. J.* **1991**, *60*, 1315−1325.
(38) Arleth, L.; Bauer, R.; Øgendal, L. H.; Egelhaaf, S. U.; Schurtenberger, P.; Pedersen, J. S. Growth behavior of mixed wormlike micelles: a small-angle scattering study of the lecithin−bile salt system. *Langmuir* **2003**, *19*, 4096−4104.
(39) Mazer, N. A.; Carey, M. C.; Kwasnick, R. F.; Benedek, G. B. Quasielastic light scattering studies of aqueous biliary lipid systems. size, shape, and thermodynamics of bile salt micelles. *Biochemistry* **1979**, *18*, 3064−3075.
(40) Pedersen, J. S.; Egelhaaf, S. U.; Schurtenberger, P. Formation of polymerlike mixed micelles and vesicles in lecithin-bile salt solutions: a small-angle neutron-scattering study. *J. Phys. Chem.* **1995**, *99*, 1299−1305.
(41) Shankland, W. The equilibrium and structure of lecithin-cholate mixed micelles. *Chem. Phys. Lipids* **1970**, *4*, 109−130.

DOI: 10.1021/acs.langmuir.5b03267
Langmuir 2015, 31, 13312−13320

(42) Tung, S.-H.; Huang, Y.-E.; Raghavan, S. R. A new reverse wormlike micellar system: mixtures of bile salt and lecithin in organic liquids. *J. Am. Chem. Soc.* **2006**, *128*, 5751−5756.
(43) Lee, H.-Y.; Diehn, K. K.; Ko, S. W.; Tung, S.-H.; Raghavan, S. R. Can simple salts influence self-assembly in oil? multivalent cations as efficient gelators of lecithin organosols. *Langmuir* **2010**, *26*, 13831−13838.
(44) Reinhold, J. G.; Ferguson, L. K.; Hunsberger, A. The composition of human gallbladder bile and its relationship to cholelithiasis. *J. Clin. Invest.* **1937**, *16*, 367−382.
(45) Mackay, C.; Crook, J. N.; Smith, D. C.; McAllister, R. A. The composition of hepatic and gallbladder bile in patients with gallstones. *Gut* **1972**, *13*, 759−762.
(46) Foldvari, M.; Gesztes, A.; Mezei, M. Dermal drug delivery by liposome encapsulation: clinical and electron microscopic studies. *J. Microencapsulation* **1990**, *7*, 479−489.
(47) Fresta, M.; Puglisi, G. Application of liposomes as potential cutaneous drug delivery systems. in vitro and in vivo investigation with radioactively labelled vesicles. *J. Drug Targeting* **1996**, *4*, 95−101.
(48) Cully, M. Inflammatory diseases: hydrogel drug delivery for inflammatory bowel disease. *Nat. Rev. Drug Discovery* **2015**, *14*, 678−679.
(49) Lalitha, K.; Prasad, Y. S.; Maheswari, C. U.; Sridharan, V.; John, G.; Nagarajan, S. Stimuli responsive hydrogels derived from a renewable resource: synthesis, self-assembly in water and application in drug delivery. *J. Mater. Chem. B* **2015**, *3*, 5560−5568.
(50) Wu, J.; Chen, A.; Qin, M.; Huang, R.; Zhang, G.; Xue, B.; Wei, J.; Li, Y.; Cao, Y.; Wang, W. Hierarchical construction of a mechanically stable peptide-graphene oxide hybrid hydrogel for drug delivery and pulsatile triggered release in vivo. *Nanoscale* **2015**, *7*, 1655−1660.
(51) Xue, B.; Kozlovskaya, V.; Liu, F.; Chen, J.; Williams, J. F.; Campos-Gomez, J.; Saeed, M.; Kharlampieva, E. Intracellular degradable hydrogel cubes and spheres for anti-cancer drug delivery. *ACS Appl. Mater. Interfaces* **2015**, *7*, 13633−13644.
(52) Jeng, U.-S.; Su, C. H.; Su, C.-J.; Liao, K.-F.; Chuang, W.-T.; Lai, Y.-H.; Chang, J.-W.; Chen, Y.-J.; Huang, Y.-S.; Lee, M.-T.; Yu, K.-L.; Lin, J.-M.; Liu, D.-G.; Chang, C.-F.; Liu, C.-Y.; Chang, C.-H.; Liang, K. S. A small/wide-angle x-ray scattering instrument for structural characterization of air-liquid interfaces, thin films and bulk specimens. *J. Appl. Crystallogr.* **2010**, *43*, 110−121.
(53) Kline, S. R. Reduction and analysis of SANS and USANS data using IGOR pro. *J. Appl. Crystallogr.* **2006**, *39*, 895−900.
(54) Nallet, F.; Laversanne, R.; Roux, D. Modelling X-ray or neutron scattering spectra of lyotropic lamellar phases: interplay between form and structure factors. *J. Phys. II* **1993**, *3*, 487−502.
(55) Berghausen, J.; Zipfel, J.; Lindner, P.; Richtering, W. Influence of water-soluble polymers on the shear-induced structure formation in lyotropic lamellar phases. *J. Phys. Chem. B* **2001**, *105*, 11081−11088.
(56) Egerton, R. F.; Li, P.; Malac, M. Radiation damage in the TEM and SEM. *Micron* **2004**, *35*, 399−409.
(57) Thyse, E. L.; Akdogan, G.; Olivier, E. J.; O'Connell, J. H.; Neethling, J. H.; Taskinen, P.; Eksteen, J. J. 3D insights into nickel converter matte phases: direct observations via TEM and FIB SEM tomography. *Miner. Eng.* **2013**, *52*, 2−7.
(58) Fairhurst, D.; Ribitsch, V. Zeta potential measurements of irregular shape solid materials. *Particle Size Distribution II, ACS Symposium Series* **1991**, *472*, 337−353.
(59) Thielbeer, F.; Donaldson, K.; Bradley, M. Zeta potential mediated reaction monitoring on nano and microparticles. *Bioconjugate Chem.* **2011**, *22*, 144−150.
(60) Kraemer, E. O.; Dexter, S. T. The light-scattering capacity (tyndall effect) and colloidal behavior of gelatine sols and gels. *J. Phys. Chem.* **1926**, *31*, 764−782.
(61) Coello, A.; Meijide, F.; Núñez, E. R.; Tato, J. V. Aggregation behavior of bile salts in aqueous solution. *J. Pharm. Sci.* **1996**, *85*, 9−15.
(62) Seth, M.; Ramachandran, A.; Murch, B. P.; Leal, L. G. Origins of microstructural transformations in charged vesicle suspensions: the crowding hypothesis. *Langmuir* **2014**, *30*, 10176−10187.
(63) Dobrynin, A. V.; Rubinstein, M. Theory of polyelectrolytes in solutions and at surfaces. *Prog. Polym. Sci.* **2005**, *30*, 1049−1118.
(64) Martin, F. J.; MacDonald, R. C. Phospholipid exchange between bilayer membrane vesicles. *Biochemistry* **1976**, *15*, 321−327.
(65) Nichols, J. W.; Pagano, R. E. Kinetics of soluble lipid monomer diffusion between vesicles. *Biochemistry* **1981**, *20*, 2783−2789.
(66) Bergmeier, M.; Gradzielski, M.; Hoffmann, H.; Mortensen, K. Behavior of a charged vesicle system under the influence of a shear gradient: a microstructural study. *J. Phys. Chem. B* **1998**, *102*, 2837−2840.

DOI: 10.1021/acs.langmuir.5b03267
Langmuir 2015, 31, 13312−13320